Positioning Annihilation Photon Interactions in a Thin LSO Crystal Sheet with a Position-Sensitive Avalanche Photodiode

Angela M K Foudray, *Student Member, IEEE*, Frezghi Habte, *Member, IEEE*, Craig S Levin, *Member, IEEE*, Peter D Olcott, *Member, IEEE*

***Abstract*—Using scintillation crystal sheets instead of discrete crystal arrays in high-resolution PET has the advantage of reduced complexity. In order to evaluate the positioning capability of a position sensitive avalanche photodioide (PSAPD) using a sheet Lutetium Oxyorthosilicate (LSO) crystal scintillator, we need to understand the functional dependence of a detected event position on the known source position. We studied positioning with both collimated 57Co 122keV and coincidence-triggered 22Na 511keV sources, which were stepped across the face of an 8mm x 8mm LSO sheet crystal coupled to an 8mm x 8mm PSAPD at 160µm intervals using a voltage-driven mechanical stage with a LabVIEW controlled acquisition system. We analyze the energy resolution, sensitivity, photopeak position and energy gated full width at half maximum (FWHM) spread of the detected position for a particular known source position. We have observed a 10% variation in average energy from the center of the crystal to the edge with 57Co and <1% for 22Na and an average point spread function FWHM of 2.86mm and 1.12mm for 57Co and 22Na respectively. We investigated methods to create a 1-1 map between (1) the four positioning signals from the PSAPD and the recorded energy and (2) the true position of the annihilation photon interaction. We found the average energy change over the 1.2mm near the edge of the continuous LSO crystal to be ~5% - insufficient to resolve with the prototype PSAPD (energy resolution 12%) with an Anger-type logic positioning algorithm. Simulation using the annihilation photon interactions from GATE and scintillation photon transport from DETECT2000 have confirmed the effects observed in experiment.**

I. Introduction

We are developing a high-sensitivity, high-resolution small animal positron emission tomography (PET) system for studying the kinetics and mechanisms of human disease in small laboratory animal models. Most high-resolution imaging systems in use and in development are incorporating increasingly smaller pixilated scintillation crystals to try to improve system resolution. Using a thin, continuous crystal may provide increased resolution while decreasing complexity and costs associated with crystal cutting, surface preparation and detector system assembly. Experimental and simulated results show comparable position resolution in the center 6mm of the device using a continuous crystal as compared to a 1mm pixellated array, with degeneracy at the edges using anger-logic type positioning.

a)

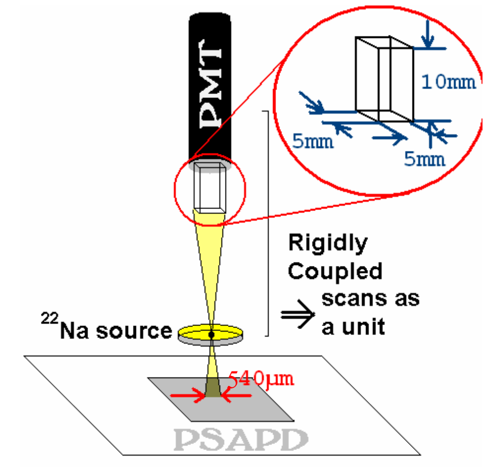

b)

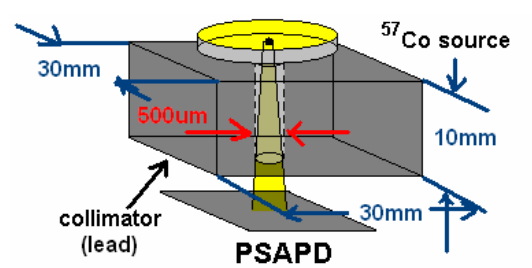

Fig. 1. The acquisition setup for a) coincidence-collimated ^{22}Na annihilation photon detection and b) lead collimated ^{57}Co gamma photon detection.

Manuscript received October 31, 2004. This work was supported in part by grant #R21 EB003283 from NIH-NIBIB.

Angela M K Foudray is a graduate student at the University of California – San Diego, La Jolla, CA USA and is working at Stanford University, Palo Alto, CA USA (telephone: 650-736-2598, e-mail: afoudray@stanford.edu).

Frezghi Habte is with Stanford University, Palo Alto, CA USA (e-mail: fhabte@stanford.edu)

Craig S Levin is with Stanford University, Palo Alto, CA USA (e-mail: cslevin@stanford.edu)

Peter D Olcott is with Stanford University, Palo Alto, CA USA (e-mail: pdo@stanford.edu)

II. Experimental Study

A. Setup

The PSAPD being characterized is a prototype developed by RMD, Inc. with an active region of 8mm x 8mm (see figure 2). A 8mm x 8mm x 1mm LSO sheet crystal is coupled to the PSAPD with silicone optical grease in each experiment. Seven layers of Teflon were wrapped around the crystal for a reflective coating. A LabView controlled, motorized MM-4M-EX-140 micro-stage from National Aperture was used to automate and accurately control the steps across the detector. Two sources were used to observe the point spread function and positioning linearity of the PSAPD: ^{57}Co with gamma photon energies of 122 keV and 22Na with annihilation photon energies of 511 keV. To collimate the highly energetic 511 keV photons from the 22Na source, a coincidence setup was employed (see the top of figure 1). A Hamamatsu H3164 photomultiplier tube (PMT) was coupled to a Teflon-wrapped 5mm x 5mm x 10mm LSO crystal with silicone optical grease. The PMT was mechanically coupled to the source at a distance of 190mm and moved with the micro-stage in 160µm steps. The source-PSAPD distance was kept at a constant 1.5mm. The geometry of the setup resulted in a 540µm spot size on the face of the PSAPD. The coincidence circuit comprised of Fast Filter Amplifiers, Constant Fraction Discriminators, a TAC/SCA, and Gate and Delay Generator NIM modules to trigger the four-channel PSAPD event acquisition. The ^{57}Co source was collimated using a 30mm x 30mm x 10mm block of lead with a 500µm hole (see the bottom of figure 1). Positions were calculated from the four digitized PSAPD channels using Anger-type logic. The units of position and therefore the point spread function full width at half maximum (psfFWHM), as well as the average energy, are all reported in a normalized form. Position is calculated from the four digitized voltages from the corner anodes of the PSAPD (see figure 3) in the following manner:

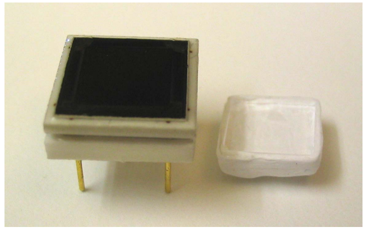

Fig. 2. An image of the PSAPD device and continuous Teflon-wrapped LSO crystal.

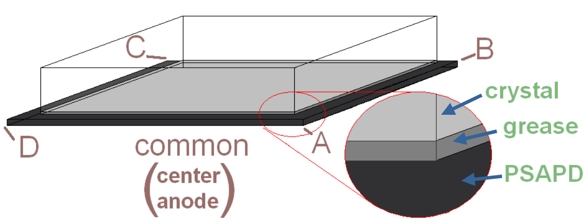

Fig. 3. A cartoon depicting anode positions used in equations (1) and (2) and layers of material used in all experiments and simulations.

$$x = \frac{(A+B)-(C+D)}{A+B+C+D} \qquad (1)$$

$$y = \frac{(B+C)-(A+D)}{A+B+C+D} \qquad (2)$$

(range: [0,5] for A, B, C and D, range: [-1,1] for x and y). The average energy is calculated from the sum A+B+C+D and has a range of [0 20]. The energies and counts plotted in figure 4 are shown at a fraction of their measured value to better visualize all data represented.

B. Tests and Results

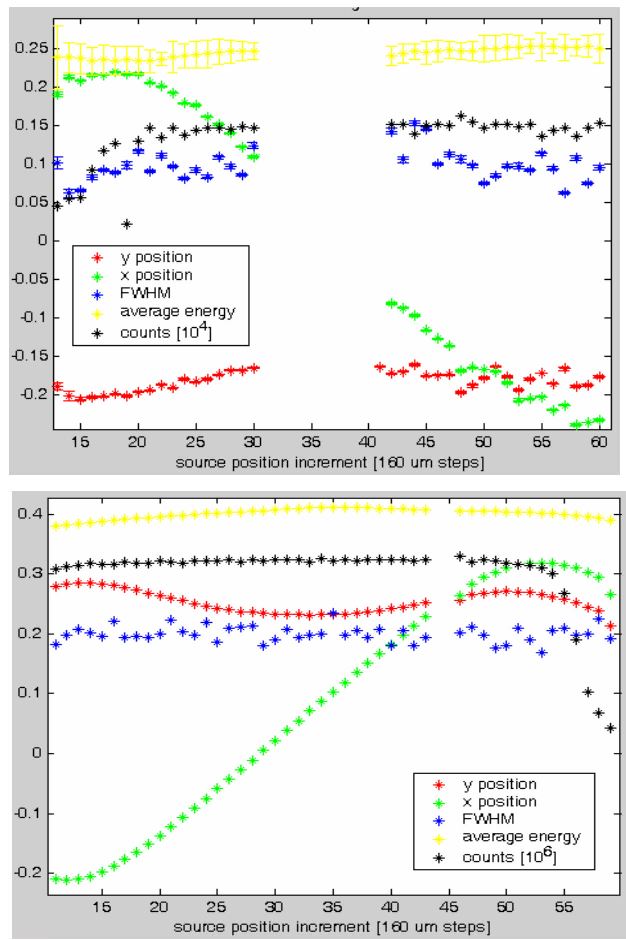

Fig. 4. For both (a) and (b): green = moving coordinate position, red = stationary coordinate position, blue = FWHM of light spread function (see figure 2), yellow = average energy, black = number of counts in the photopeak. All quantities are in normalized units. (a) ^{22}Na (b) ^{57}Co (error bars smaller than the data point symbol size)

Using the setups previously described, a 10µCi ^{22}Na and a 10µCi ^{57}Co were stepped in a line across the face of the PSAPD detector. Figure 4 shows the detected position spread for ^{22}Na (left) and ^{57}Co (right) at a particular source position. The log of the histogrammed counts are in part b) of figure 4 to show the relative size of the spread of events with respect to the size of the detection area. Data was gathered for 2000

0-7803-8700-7/04/$20.00 (C) 2004 IEEE

seconds (33 min) at each location using the ^{22}Na setup and for 120 seconds for the ^{57}Co. Although the acquisition times for the ^{22}Na setup were much longer, the number of events are much lower for this case due to the coincidence collimation method - about 1000 events after energy gating at 1/5 peak height – whereas over 30,000 events were gathered in 2 minutes, after energy gating, at each increment, using the collimated ^{57}Co source. The centroid of the positions of the events for a particular "true" location was calculated and plotted along with the number of counts and the average energy (see figure 4). The much simpler single photon setup (figure 4, left) encourages further study noting the large region of linearity to nearly the edge of the detector (points 13-52 or over 6.2mm). Noting also that the average energy does not remain constant at the edge of the detector lends a fifth positioning parameter to resolve positioning difficulties at the edge. The raw energy resolution for ^{57}Co was 24.45% +/- 0.2% and 17.33% +/- 1.06% for ^{22}Na near the center. Near the edges, the uncorrected energy resolution for ^{57}Co was 24.92% +/- 0.2% and 15.24% +/- 1.18% for ^{22}Na. The psfFWHM and position can be calculated in [mm] by the factor: 8[mm]/R where R is the full data range in normalized units. For ^{57}Co, the measured psfFHWM averages 0.2 x 8/0.55 = 2.9mm and 0.1 x 8/0.65 = 1.23mm for ^{22}Na. Deconvolving the finite size of the 500μm source using a first approximation sqrt((meas. psfFWHM)^2 - (500μm)^2) gives 2.86 for ^{57}Co and 1.12 for ^{22}Na. The positioning linearity for the central 6mm has an R^2-value of 0.965 for ^{22}Na and 0.9995 for ^{57}Co.

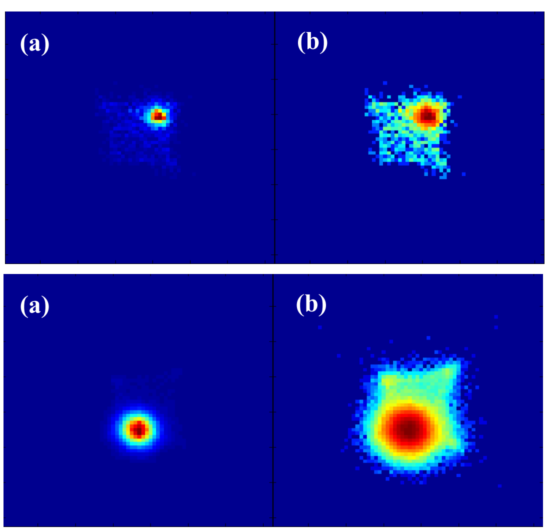

Fig. 5. For a single source position, a) the histogrammed centroid of the light spread b) the log of the histogram values (enhance the visualization of the dynamic range). Top: ^{22}Na and bottom: ^{57}Co

III. MONTE CARLO STUDY

To compare these results with theory, we utilized two standard simulation packages to model both the high and low energy interactions in the LSO scintillation crystal. The interaction mechanisms of the high-energy annihilation photon were simulated with the new medical imaging Monte Carlo add on package to the GEANT4 software, GATE. The subsequent scintillation photon transport and interaction mechanisms were carried out using the DETECT2000 package.

A. GATE

To simulate similar conditions as seen in the ^{22}Na experimental coincidence study, GATE was used to obtain Compton scatter, Photoelectric and characteristic X-ray interaction positions in the LSO scintillation crystal. A 20μm radius sphere was placed 5mm from the surface of an 8mm x 8mm x 1mm single LSO crystal, which emitted 511keV photons normal to the surface of the crystal (see figure 6).

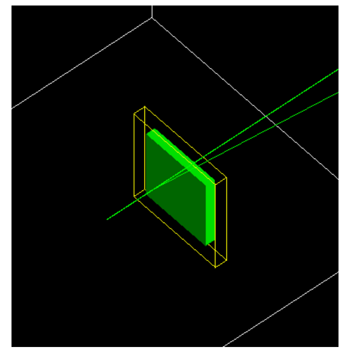

Fig. 6. A screen shot during GATE simulation. The green lines are photons. Left of the green crystal is the origin of the source, to the right, the transmitted photons.

Each interaction with the crystal is recorded by GATE into a "hits" file, which gives a great deal of information including the energy, three-dimensional position, and original annihilation event number. In order to probe the location-dependent response and light spread, the source sphere was stepped at 200μm increments at the locations of the face of the detector shown figure 7 in red. The position, energy and event number were passed, for each "hits" interaction to DETECT2000 to simulate optical transport within the crystal.

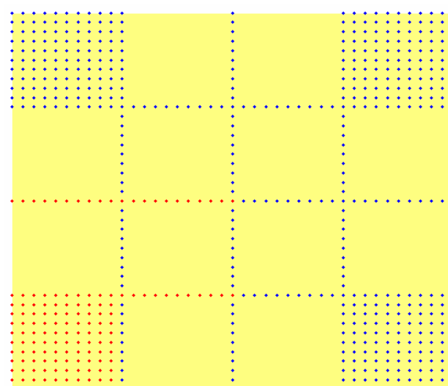

Fig. 7. The positions that were simulated are in red. The behavior at the blue positions is known by symmetry of the PSPAD device.

B. DETECT2000

The interactions determined by GATE were modeled as a point process, i.e., the scintillation photons modeled by DETECT2000 for a particular GATE interaction ("hit") were all given the same initial location, the one listed in the "hits" file. DETECT2000 requires for input a location and number of

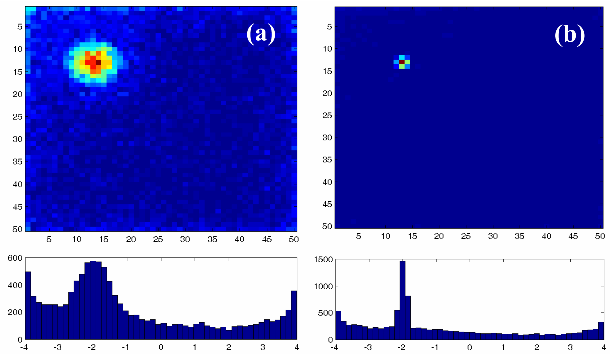

Fig. 8. (a) 2D and 1D histogram of the individual scintillation photons from one “hits” interaction which originated 0.63 mm from the bottom of the crystal. (b) an interaction from the same x,y position and energy as (a) but 0.16 mm from the bottom of the crystal.

photons to generate and outputs for each scintillation photon a location. The event number was passed through each step of the simulations to keep together all interactions and subsequent scintillation photons from the same event. The energy given in the GATE “hits” file was converted to a number of photons to generate for the DETECT2000 step using the average LSO value of 25 photons per keV. The two materials simulated are shown in figure 2: an 8mm x 8mm x 1mm LSO crystal, with index of refraction 1.82, and a 10µm deep optical grease layer

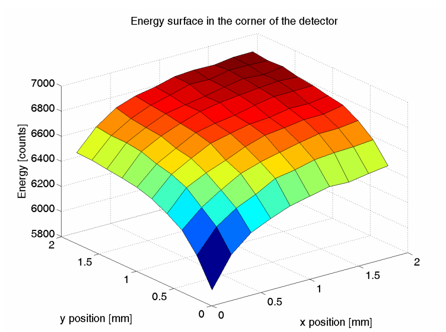

Fig. 9. Average energy at locations in the corner of the PSAPD.

with the same cross-section and an index of refraction of 1.465. The surface finish on the five faces of the scintillation crystal not in contact with the optical grease were considered ground, and the sixth connecting face, polished. These surface definitions were mirrored in the grease layer, except for the side considered in contact with the PSAPD which was defined as the detect layer. Scintillation photons that come in contact with this detect layer are considered detected and the position and location are automatically written out. The position reported is the mean of the centroids of the photons from an event. The PSAPD resistive surface was not modeled to simulate pincushion effects, which add non-linear distortions in these position estimates. These effects are small in this detector in the location that the experimental data were taken, i.e., the pincushion effect is not large where the experimental data was taken [1]. There is a larger region over which the calculated position for the 122keV ^{57}Co data is non-linear due to the larger spot size and that more of the interactions happen closer to the top of the crystal (farther from the detector surface – see figure 8).

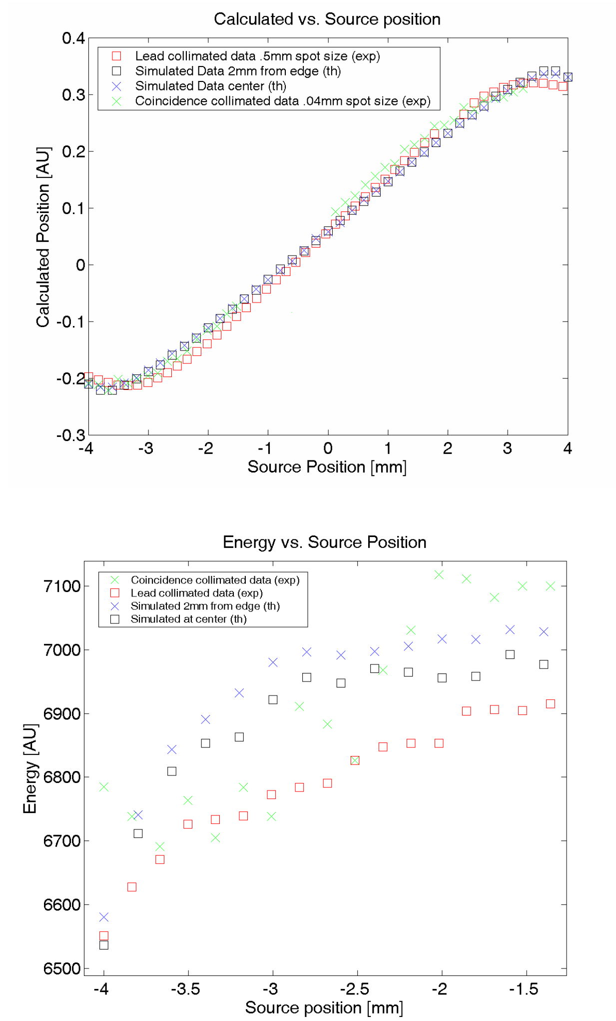

Fig. 10. (a): comparison of experimental (exp) and simulated (th) calculated position (see formula to the left), and (b): experimental (exp) and simulated (th) energy vs. source position.

IV. Conclusion

Calculated positions from events whose centroid are in the first 1.5 mm near the edge of the sheet crystal are degenerate. This is due to a sizable portion of the scintillation photons reflecting off the surface of the crystal. Because of these reflections, some photons are lost, changing the average energy of events positioned at the edge as compared to events at the center of the detector. The percentage change of this energy in the first 1.5 mm is about 5%. The energy resolution of our characterized PSAPD is 10-12%. Even with a maximum likelihood estimation for positioning, for a high sensitivity, high-resolution PET system, using a single sheet crystal, we would need a detector with better than 5% energy resolution to out-perform position sensitive detectors coupled to single crystals using Anger-logic type positioning and energy information. Further efforts to utilize all the information collected from the four anode channels could involve maximum-likelihood estimation algorithms. Using Anger-type logic alone, this loss of resolution near the edge of the crystal is a price that may be considered since it drastically increases sensitivity due to higher packing fraction and more preferable crystal placement [5].

V. Acknowledgment

The authors would like to acknowledge D. Farrel, M. McClish, M. Squillante, and K. Shah at RMD, Inc. for their ideas and support.

VI. References

[1] C.S. Levin, A.M.K. Foudray, P.D. Olcott, F. Habte. "Investigation of Position Sensitive Avalanche Photodiodes for a New High Resolution PET Detector Design." *IEEE Transactions on Nuclear Science 51 (3) 805 – 810, June 2004*

[2] C.S. Levin, AMK Foudray, et al, "Impact of High Energy Resolution Detectors on the Performance of a PET System Dedicated to Breast Cancer Imaging." *Oral Presentation at the 2004 IEEE Breast Imaging Workshop, Oct 22-23, 2004, Roma, Italy*

[3] C.S. Levin, F. Habte, and A.M. Foudray. "Methods to Extract More Light from Minute Scintillation Crystals Used in an Ultra-High Resolution Positron Emission Tomography Detector." *Nuclear Instruments and Methods in Physics Research Section A (in press, 2004)*.

[4] C.S. Levin, R. Farrell, AMK Foudray, et al., "A Thin Position Sensitive Avalanche Photodiode Has Been Fabricated for Ultra-High Resolution PET to Achieve Robust Scintillation Light Collection Efficiency with High Crystal Packing Fraction" *Presented at 2004 IEEE Medical Imaging Conference, Oct 16-22, Roma, Italy*

[5] Foudray, AMK, et al., "Optimization of a Cylindrical PET Breast Imaging System Comprised of Position Sensitive Avalanche Photodiodes Utilizing Monte Carlo Simulation" *Presented at the 2004 IEEE Breast Imaging Workshop, Oct 22-23, 2004, Roma, Italy*